EVALUATION OF MICROSTRUCTURES, MECHANICAL AND DRY-SLIDING WEAR PERFORMANCE OF A356-(FLY ASH/SICP) HYBRID COMPOSITES

R. Soundararajan, A. Sathishkumar, G. Shanthosh and S. Karthik
Department of Mechanical Engineering, Sri Krishna College of Engineering and Technology, Coimbatore, India

S. Sivasankaran
Department of Mechanical Engineering, College of Engineering, Qassim University, Buraydah, Kingdom of Saudi Arabia

https://doi.org/10.1007/s40962-021-00731-3

Abstract

The present study was conducted to examine the physical, metallurgical, mechanical, and tribological behaviors of A356 alloy reinforced with fly ash (5, 10 wt%), and SiCp (2.5 wt%) hybrid composites. Three hybrid composites were synthesized and consolidated through a stir cum squeeze cast technique followed by solution treatment and aging. X-ray diffraction and microstructural evaluations were performed using an optical microscopy and a scanning electron microscopy. The microstructural results revealed pore-free, homogeneous dispersions and effective bonding of reinforcements in the matrix. The experimental bulk density of the A356-10wt% fly ash-2.5 wt% SiC hybrid composite exhibited lower value compared with other samples indicating lighter weight. The same sample produced Brinell hardness number of 90.35 ± 3.80 HB and ultimate strength of 329 MPa which was 1.28 times and 1.14 times higher than matrix respectively. The dry sliding wear test results showed that the wear rate and coefficient of friction started to increase with increasing applied load and sliding speed. The 10 wt% fly ash sample produced lower wear rate 1.42 × 10^{-3} mg/m at a load 10 N and sliding distance of 1000 m. Finally, the surface worn-out mechanisms were studied using SEM. The developed 10 wt% fly ash-based hybrid composite exhibited improved performances recommending to use in automotive and various structural parts.

Keywords: *hybrid composites, stir cum squeezed, physical, metallurgical, mechanical, tribological behavior*

Introduction

Aluminum matrix composites (AMCs) are commonly used in several sectors (automotive parts, aircraft, missile parts, and structural components) owing to their high strength-to-weight ratio, high stiffness, light weight, mechanical properties, wear resistance, and controlled coefficient of thermal expansion.[1] Al alloys have inadequate strength and are insufficient for replacing the present automobile components made from high density materials.[2] The dispersion of more than one reinforcement phase is possible which can be a particulate form, continuous fiber form, or discontinuous whisker form to improve the performance of Al matrix alloys.[3] The incorporation of more than one conventional ceramic reinforcement in an Al matrix increases the cost.[4] Some reinforcements obtained from industrial wastes, and agro wastes are alternative choices that can also improve the mechanical performance of Al-based composites, and save the environment.[5] Hybrid metal matrix composites (HMMCs) are fabricated by incorporating more than one reinforcement particle in a single continuous ductile matrix to increase the strength, and stiffness compared to a single reinforcement of AMCs.[6] Aluminum-silicon (Al-Si) alloy-based composites have become common owing to their unique properties. Almost all ceramic reinforcements are compatible with these alloys owing to their excellent castability.[7] Among the various existing reinforcements, low-cost waste fly ash can also be used as reinforcement owing to its low density leading which reduces the structural component weight, is available at low cost or free of cost, and decreases the life cycle

Received: 10 September 2021 / Accepted: 21 November 2021 / Published online: 13 January 2022

cost of products.[8] Furthermore, the incorporation of fly ash particles with aluminum alloy increases hardness, stiffness with damping properties, and wear resistance.[9] Silicon carbide particles (SiCp) are composed of tetrahedral carbon followed by silicon atoms with a better interconnect in the crystal lattice. In addition to increasing the strength of the matrix, SiCp provides a strong material structure and significantly improves the tribological, mechanical, and thermal properties.[10] The industrial demand for high strength and low wear rate in HMMCs is dependent on the reinforcement phase and processing techniques. A356 hybrid composites with SiC and fly-ash particles processed via electromagnetic stir casting yielded the best results because of the presence of 5wt% fly ash.[11] Hybrid reinforcements of B_4C and fly ash particles (each 4 wt% addition) with the A356 matrix processed through the stir casting technique demonstrated significant growth in mechanical and tribological properties owing to the uniform particle distribution in the matrix.[12] An A356 alloy-based hybrid composite was produced via a compo casting process by incorporating Al_2O_3, SiC ceramic particles, and graphite particles. The use of SiC particulates yielded a better response than Al_2O_3 particulate composites, and the addition of graphite particles improved the tribological properties owing to its solid lubricant characteristics.[13] Substantial research on metal matrix composites (MMCs) has been performed using Al_2O_3, SiC, B_4C, Gr, AlN, TiB_2, and ZrO_2 particles with various grades of aluminum alloys to achieve their unique properties by varying the weight percentages of reinforcements via the stir casting technique mostly.[14–20] Stir casting, electromagnetic stir casting, spray casting, compo casting, and pressure-less metal infiltration techniques are commonly used to fabricate AMCs. Among these techniques, the stir casting technique is a simple processing route for manufacturing AMCs because of the random scattering of the reinforced particles within the matrix; however, poor bonding of incorporated ceramic particles over the matrix is a major issue in stir casting.[21] On the other hand, the stir cum squeeze cast technique for preparing AMCs eliminates micro porosities while maintaining good bonding and high strength.[22] The need for improved tribological properties in AMCs is important in industrial applications during reinforcement addition in the matrix.[23] Reinforcement of alumina (Al_2O_3) and graphite (Gr) particles with Al-Si-10Mg alloy was processed through a stir casting route to evaluate the behavior under dry sliding conditions. A tribometer setup was utilized to note the responses, such as the rate of wear and frictional coefficient by fluctuating the applied load, speed of the disc under constant sliding distance conditions. The rate of wear and frictional coefficient decreased as the sliding speed and loading conditions increased.[24] A356 composites containing 20% SiC particulates were investigated using the compo cast route. The responses revealed that the treated SiC particles had less abrasion and adhesion on the worn surface than the cast SiC particles, which have undergone severe abrasion and delamination due to poor bonding.[25] The Al alloy reinforced with 2 wt% B_4C and different wt% fly ash (varied from 5 to 20 wt%) processed using stir casting technique has confirmed that upto15 wt% fly ash addition increases the tensile and yield properties, but decreased the extension while increasing the hardness. The wear rate results were found to be lower in the metal matrix containing 20 wt% fly ash than in other composite samples.[26] A356 alloy with a higher quantity of Al_2O_3 and multi-wall carbon nanotube (MWCNT) hybrid composites exhibit improved wear and friction performances owing to their unique mechanical strength.[25–27] According to the literature survey, the hybrid composites behavior is primarily influenced by the type of reinforcements, introduced weight/volume fraction of ceramic particles in the primary phase and method of casting process, etc. So far there is not an exact way of providing a sufficient research outcome for a specific one. Owing to the urge, the industry needs an economic method of fabrication of Al-based hybrid composites with low-cost reinforcement particles. To overcome such issues, the proposed work was formulated and studied. Furthermore, little research has been conducted on the various behaviors of squeeze cast A356 alloy and squeeze cast A356 hybrid composite incorporated with two different weight percentages of fly ash (5, and 10 wt%) and 2.5 wt% SiC have not been explored. The primary objective of this study was to explore the physical, metallurgical, mechanical, and tribological behavioral aspects which are presented in the following sub-sections. Furthermore, the contribution of fly ash particles to the improved properties of A356 alloy-2.5 wt% SiC composite was established through this work.

Materials and Methods

Matrix Material

The comparatively soft nature of the matrix material was a silicon-based hypoeutectic A356 alloy with a density of 2.67 g/cm^3 which was selected for this research work. The chemical composition of the as-received A356 ingots is

Table 1. Chemical Composition of As-Received A356 Ingot Alloy

Element	Cu	Mg	Si	Ti	Mn	Zn	Fe	Traces	Al
Wt%	0.2	0.4	7.5	0.20	0.1	0.1	0.2	0.15	Balance

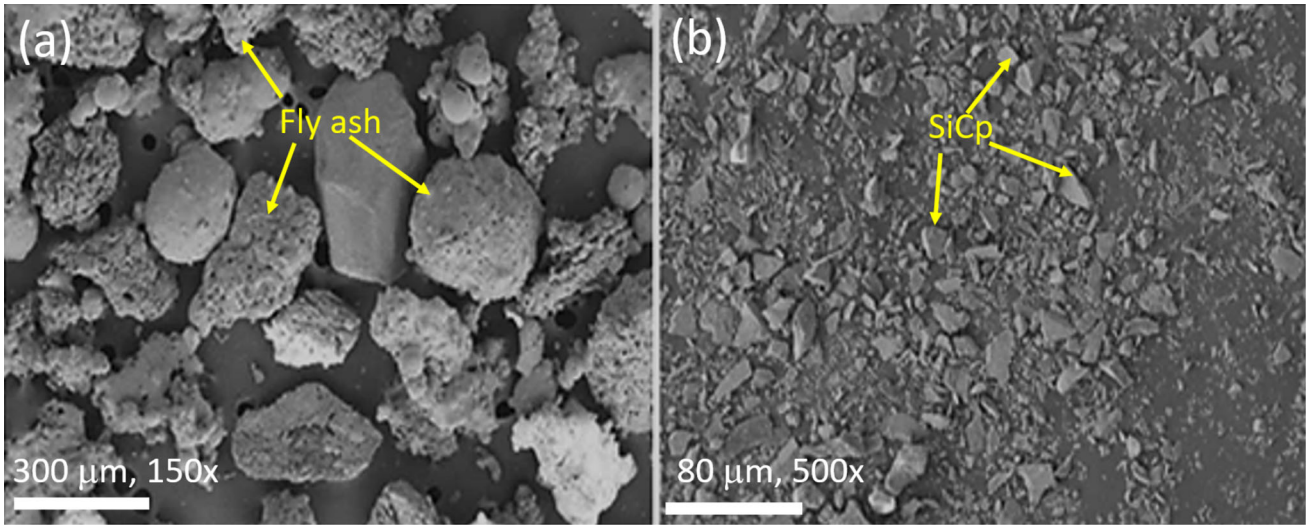

Figure 1. SEM microstructures of as-received powders: (a) fly ash at ×150; (b) Silicon carbide at 500x.

listed in Table 1. This A356 alloy matrix was selected because it is easy to cast and is widely used in a variety of applications including machine parts, vehicles, aircraft, missile components, and structural parts.[1]

Filler Materials

Filler materials are typically intermittent, harder, and more durable when dispersed in matrix materials. The addition of filler materials is usually carried out primarily to enhance the performance of MMCs. Fly-ash has a density of 2.8 g/cm^3 (given by the supplier) and is an even more cost-effective reinforcement. Fly ash can be found in massive quantities in the form of solid (precipitate) or hollow (cenosphere) particles of solid waste in thermal power plants. As the filler material, silicon carbide particles (SiCp, density of 3.21 g/cm^3) is popular reinforcement for Al-based MMCs owing to hard, and brittle ceramic particles. SiCp possesses a high modulus of elasticity, high strength, and high thermal and electrical resistances.[27] Figure 1 depicts the SEM microstructure of the procured fly ash and SiC particles with average particle sizes of 320 µm and 25 µm respectively used to prepare the hybrid composites. The size range of fly ash particles ranged from 55 to 440 µm. The size range of the SiCp ranged from 3 to 42 µm. The incorporated fly ash and silicon carbide reinforcements in the A356 alloy can enhance the physical and mechanical properties with a low density of the prepared hybrid composites. In this study, two different weight percentages of fly ash particles (5, and 10 wt%), and 2.5 wt% of SiCp were incorporated in A356 alloy. The theoretical density was calculated using the rule of mixture for the designed A356 alloy, A356-5 wt% fly ash-2.5 wt% SiCp, and A356-10 wt% fly ash-2.5 wt% SiCp hybrid composites is illustrated in Table 2. The weight percentages of incorporated elements were converted to volume fractions and then, applied the rule of mixture for determining the theoretical density.

Method of Casting Fabrication

In this study, the stir cum squeeze casting technique was used to create pore-free, evenly distributed, well-bonded sound hybrid composites. First, the A356 alloy was heated to 725°C in a steel vessel of a stir casting furnace attached to a squeeze casting set-up and allowed to achieve a homogeneous liquid phase. Subsequently, the A356 melt was degassed to remove the trapped gases and impurities from the molten metal. The molten melt was then transferred to a 255°C preheated die and allowed to solidify

Table 2. Hybrid Composite Designed Samples, Theoretical Density, Experimental Density, and Relative Density

Samples	Theoretical Density, g/cm^3	Experimental Density, g/cm^3	Relative density	Secondary dendritic arm spacing (SDAS), µm
A356 alloy	2.67	2.65 ± 0.012	0.993 ± 0.0021	150.5 ± 7.85
A356 + 5 wt% fly ash + 2.5 wt% SiC	2.47	2.44 ± 0.013	0.988 ± 0.0024	73.6 ± 5.7
A356 + 10 wt% fly ash + 2.5 wt% SiC	2.38	2.35 ± 0.011	0.987 ± 0.0020	38.4 ± 4.5

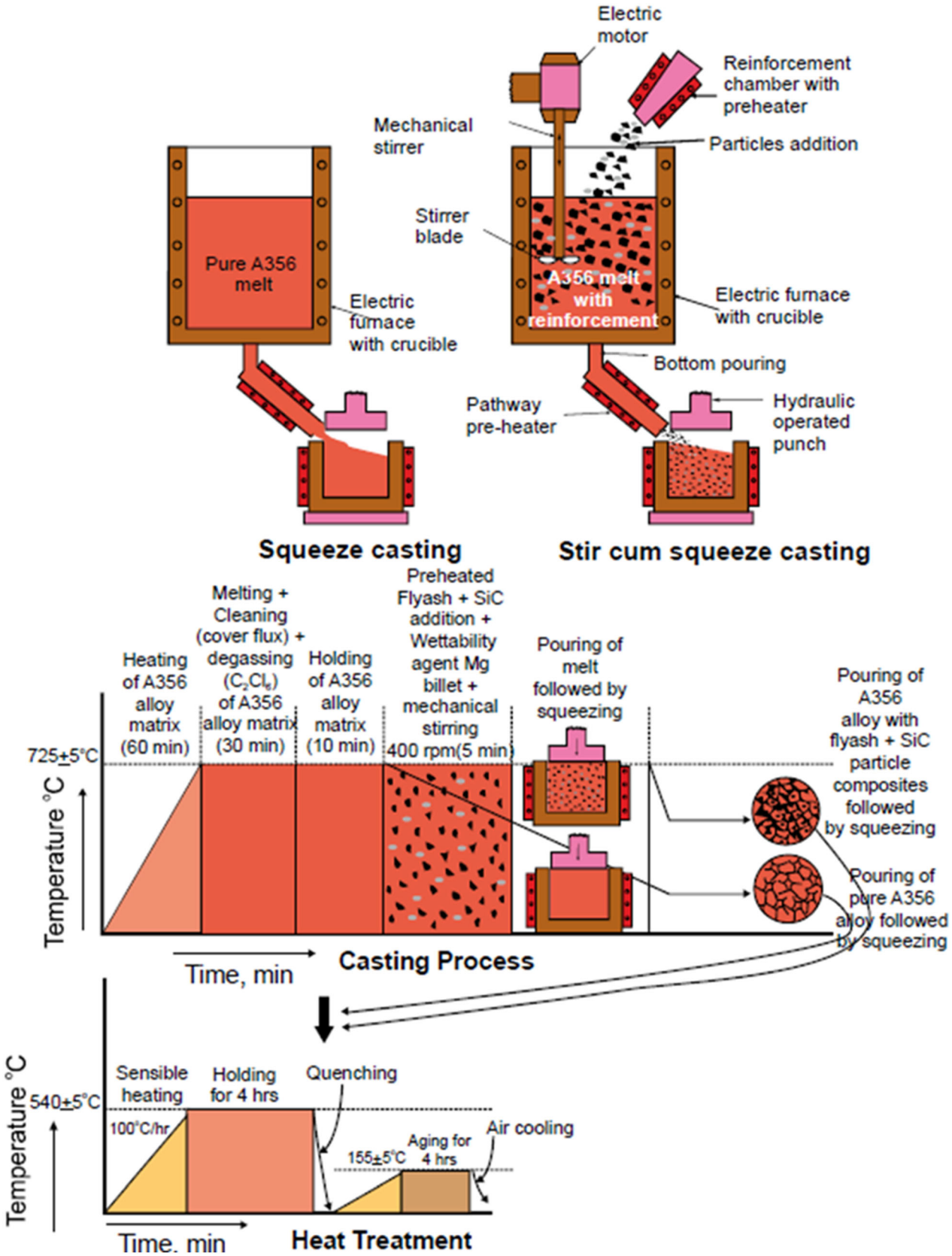

Figure 2. The schematic view illustrates squeeze casting, stir cum squeeze casting phases, and heat treatment phases.

under squeeze pressure (140 MPa) to produce a pure A356 alloy as shown in Figure 2. In the next samples, the preheated reinforcement particles of 5 wt% fly ashes, 2.5 wt% SiC, and 1 g magnesium (as a wettability agent, 0.1% for 1000 g of A356 alloy matrix) was added to the matrix melt. Further, the added reinforcements were mechanically stirred at 400 rpm for 5 min to form a fine vortex, and the ability of the fly ash and SiC particles to wet with the matrix material followed by pouring into the preheated die cavity. At this instant, a squeeze pressure of 140 MPa was immediately applied to the surface of the liquid metal top in the preheated die, squeezed, and yielding sound hybrid composite samples. Similarly, 10 wt% fly ashes and 2.5 wt% SiC hybrid reinforcements along with 0.1 wt% Mg were added into liquid A350 alloy matrix melt in order to prepare another hybrid composite using the same procedure. Figure 2 shows a schematic view illustrating the squeeze casting, stir cum squeeze casting, and heat treatment processes (solutionizing, and ageing). The stir cum squeeze casting setup is depicted in Figure 3a. The A356 ingot and cast samples are shown in Figure 3b.

Post-processing of cast samples is essential to eliminate internal stress and modify surface strength for use in real-time applications. The squeezed A356 alloy matrix, and stir cum squeezed hybrid composite samples were subjected to solution treatment, in which the samples were kept at 540°C for 4 h inside the furnace before being quenched under ambient conditions. Later, the solution-treated samples were kept at 155°C for 4 h and then cooled in air. Finally, the treated cast samples were subjected to mechanical testing and characterization.

Testing of Casted Samples

As shown in Figure 4, the cast samples were prepared with standard dimensions for physical, metallurgical, mechanical, and tribological testing. The Archimedes theory (ASTM B962-13) was used to establish the experimental densities of the cast samples. X-ray diffraction, optical microscopy and SEM were used to analyze the metallurgical behavior of the prepared samples. Prepared samples were subjected to Brinell hardness and tensile tests in accordance with the ASTM E10-18 and ASTM-E8 standards, respectively (Figure 4b, c). At least five tensile samples of each composition were used and an average was used for the investigation. Similarly, after polishing, the Brinell hardness test was carried out in different locations; at least 20 readings were measured and the average value was used for examination. In addition, SEM was used to analyze the fracture morphology on the surface.

The dry sliding wear behavior of cast samples with standard dimensions of 12 mm × 12 mm × 40 mm was prepared. The tribological test was conducted using the DUCOM pin-on-disc equipment depicted in Figure 5a and the corresponding schematic is shown in Figure 5b, c.

Figure 3. Photograph of: (a) Stir cum squeeze casting setup; (b) A356 ingot and cast samples.

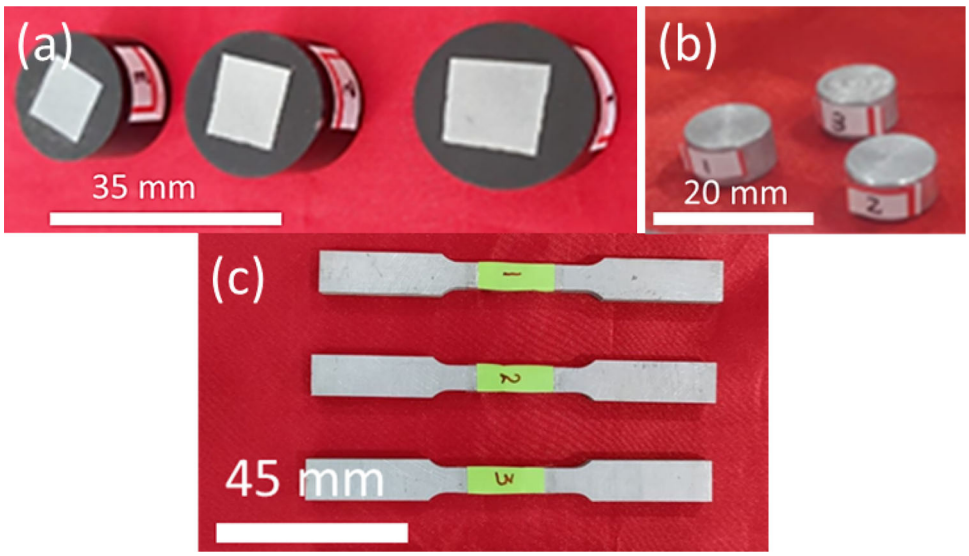

Figure 4. Prepared samples for testing (a) Metallography (b) Density and Hardness (c) Tensile tested samples.

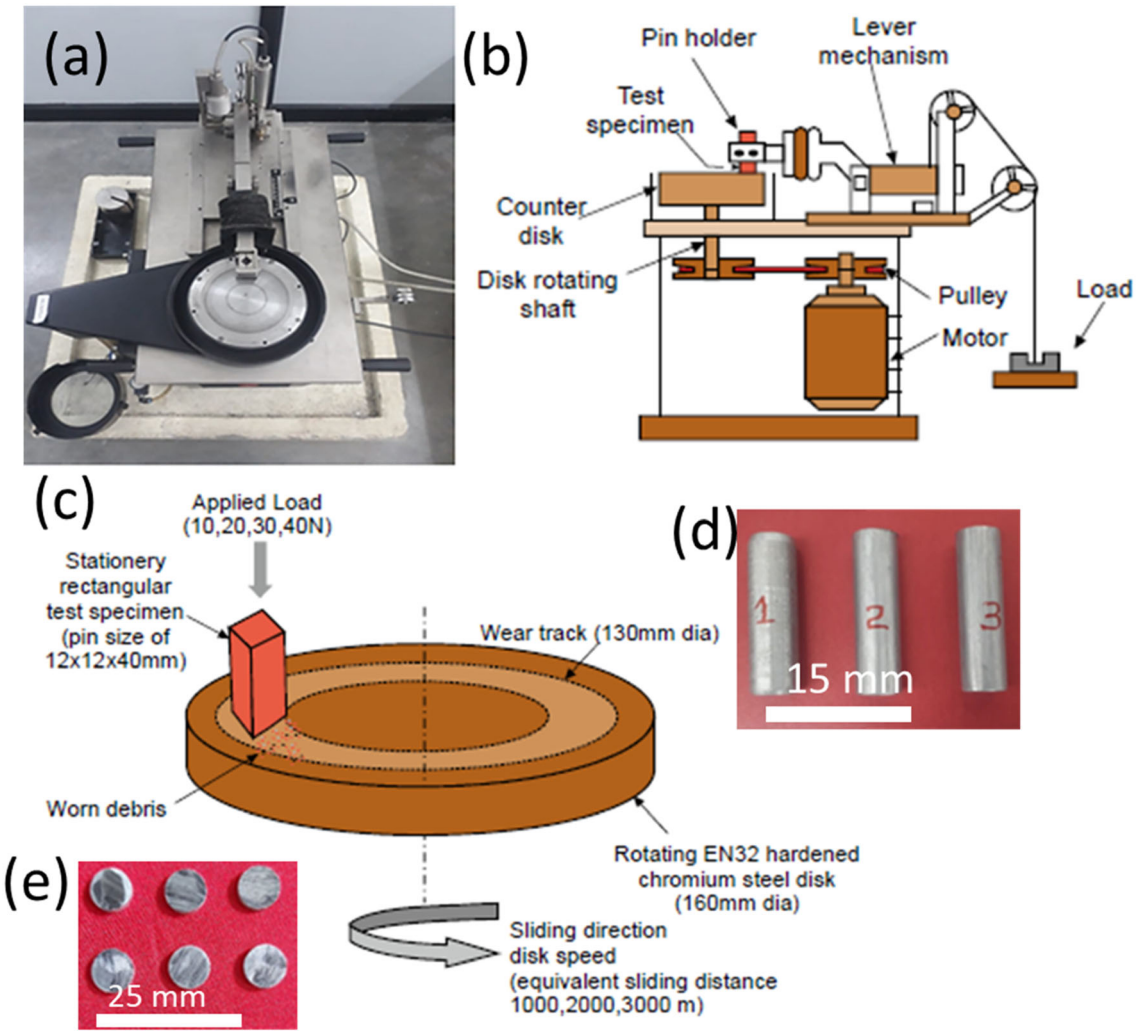

Figure 5. (a) Photograph of Pin-on-Disc tribometer equipment; (b) schematic view of pin-on-disc apparatus; (c) principle of operation of pin-on-disc method; (d) photograph of pin samples used for wear test; (e) photograph of worn-out pin surface.

Figure 5d shows the prepared cast pin specimens for tribological testing, which were held against a revolving disc of EN-32 steel material with a higher hardness value of 63 HRC. The roughness of the steel disc surface and prepared test specimens was 0.3 µm and 1.6 µm, respectively. Additionally, before the start of each test, the surfaces of the steel disc and specimens were washed with acetone. The measurements were performed under ambient conditions with a change in load conditions of 10, 20, 30, and 40 N and a sliding distance of 1000, 2000, 3000 m with equivalent sliding speeds of 1.67, 3.33, and 5 m/s, respectively, as well as fixed parameters with a time of 10 min and 130 mm track diameter. The initial and final weights of each test specimen were estimated using an electronic balance (Type ATY224) with 0.0001 g precision. The wear rate was computed by dividing the mass loss of the samples by the sliding distance. The friction force was recorded from the tribometer setup display and divided by the applied load to calculate the coefficient of friction. Five trials were performed for each prepared sample, and the average values were recorded to compute the wear rate and coefficient of friction. Figure 5e depicts a photograph of the worn pin surface of a tribometer test for examining the wear mechanism and worn surface morphology using SEM equipment.

Results and Discussion

The primary goal of the proposed research was to identify the physical, metallurgical, mechanical, and tribological behaviour of the A356 matrix, A356 with × (5, 10) wt% fly ash, and 2.5wt% SiC hybrid composite manufactured using stir cum squeeze casting followed by heat treatment. The results were correlated with each other and were clearly narrated.

Examination of Physical Properties

The lightness of the metal pieces indicates their density. The measured bulk density of squeeze cast A356 matrix, stir cum squeeze cast A356-5 wt% fly ash-2.5 wt% SiC and A356-10 wt% fly ash-2.5 wt% SiC hybrid composites was 2.65 ± 0.012 g/cm^3, 2.44 ± 0.013 g/cm^3, and 2.35 ± 0.011 g/cm^3. The theoretical density was calculated using the rule of mixture in which the experimental density was lower than the theoretical density (Figure 6), and the percentage of variance was within the acceptable limit. Owing to density differences in the reinforcement and matrix alloys, the stir cum squeezed A356 with 10 wt% fly ash and 2.5 wt% SiC hybrid composite sample possessed the lowest density. The decrease in density of the hybrid composite was due to the incorporation of fly ash particles with a low density value.[28,29] Thus, this low-density hybrid composite is expected to be environmentally and hazard-free with light weight. Additionally, the macro analysis (Figure 3b)

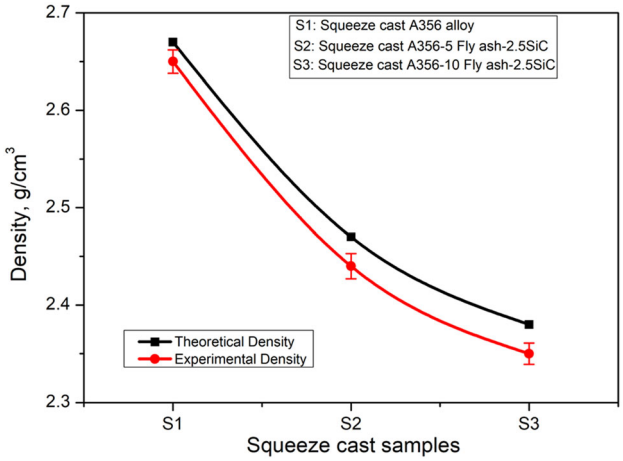

Figure 6. Variation of theoretical density and experimental density of squeeze cast A356 alloy, A356-5 wt% fly ash-2.5 wt% SiC, and A356-10 wt% fly ash-2.5 wt%SiC hybrid composites.

shows that no pores were detected as a result of the stir cum squeeze casting processing parameters used in this study.

X-ray Diffraction, and Microstructural Evaluations -Metallurgical Behavior

X-ray diffraction on squeeze cast A356 alloy, and squeeze cum stir cast A356-10 wt% fly ash-2.5SiC hybrid composite was carried out to observe the presence of various phases after heat treatment. Figure 7 shows the XRD patterns of the developed samples in which the A356 alloy sample produced α-Al and eutectic Si phases. Whereas, squeeze cum stir cast A356-10 wt% fly ash-2.5SiC hybrid composite samples exhibited α-Al, eutectic Si, SiO_2, Al_2O_3, Fe_2O_3, and SiC phases. The formation of SiO_2, Al_2O_3, and Fe_2O_3 phases is related to the incorporated fly

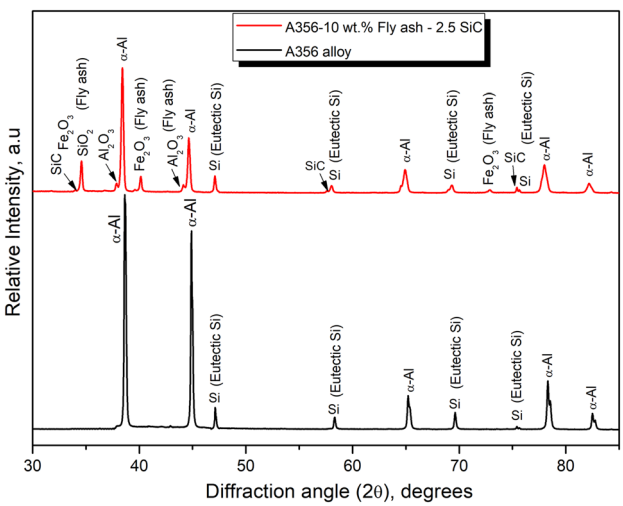

Figure 7. X-ray diffraction patterns of squeeze cast A356 alloy, and squeeze cum stir cast A356-10 wt% fly ash-2.5 wt% SiC hybrid composite.

ash particles. The peak intensity of the α-Al and eutectic Si phases decreased in the hybrid composite owing to the incorporation of fly ash and SiC particles consequently reducing the amount of the A356 matrix.[30] The results clearly explained the development of A356-10 wt% fly ash-2.5 wt%SiC hybrid composites successfully. The formation of α-Al, eutectic Si, fly ash, and SiC phases was confirmed by optical microscopy (Figure 8)[7].Figure 8a, b shows the microstructure of the squeeze cast A356 alloy with α-Al and eutectic Si phases. Figure 8c, d shows the microstructure of the stir-cum squeeze cast A356-5 wt% fly ash-2.5 wt% SiC, and A356-10 wt% fly ash-2.5wt%SiC hybrid composites, respectively. The presence of α-Al, eutectic Si, fly ash particles, and SiC particles was observed in the hybrid composites. The close observation of the optical microstructures revealed the matrix grain refinement and proper dispersion of the incorporated reinforcements.[22] ImageJ software was used to measure the secondary dendritic arm spacing (SDAS) from several optical microstructural images, and the average value was used for the investigation (Table 2). The value of SDAS decreased drastically with the incorporation of fly ash and SiC particles due to the diminishing grain growth. The SDAS values of A356-5 wt% fly ash-2.5SiC hybrid composite was 736 μm which was around two times reduced compared to A356 alloy (150.5 μm). The SDAS values of A356-10 wt% fly ash-2.5SiC hybrid composite was 38.4 μm which was around 3.9 times reduced compared to A356 alloy. The reasons for decreasing the SDAS were attributed to less space for A356 matrix growth.[1,7] The SDAS results demonstrate the drastic reduction of matrix grains by increasing the amount of fly ash particles. Enhanced mechanical behavior can be attained in hybrid composite samples when reinforcement particles are embedded and dispersed evenly. SEM microstructures were also carried out to examine the proper dispersion and embedding of the incorporated fly ash and SiC particles. Figure 9 shows the SEM images of the developed samples. The formation of α-Al and eutectic Si phases in the A356 cast is clearly shown in Figure 9a, b. SEM energy dispersive spectroscopy (EDS) was carried out to check the presence of various elements corresponding to the A356 alloy

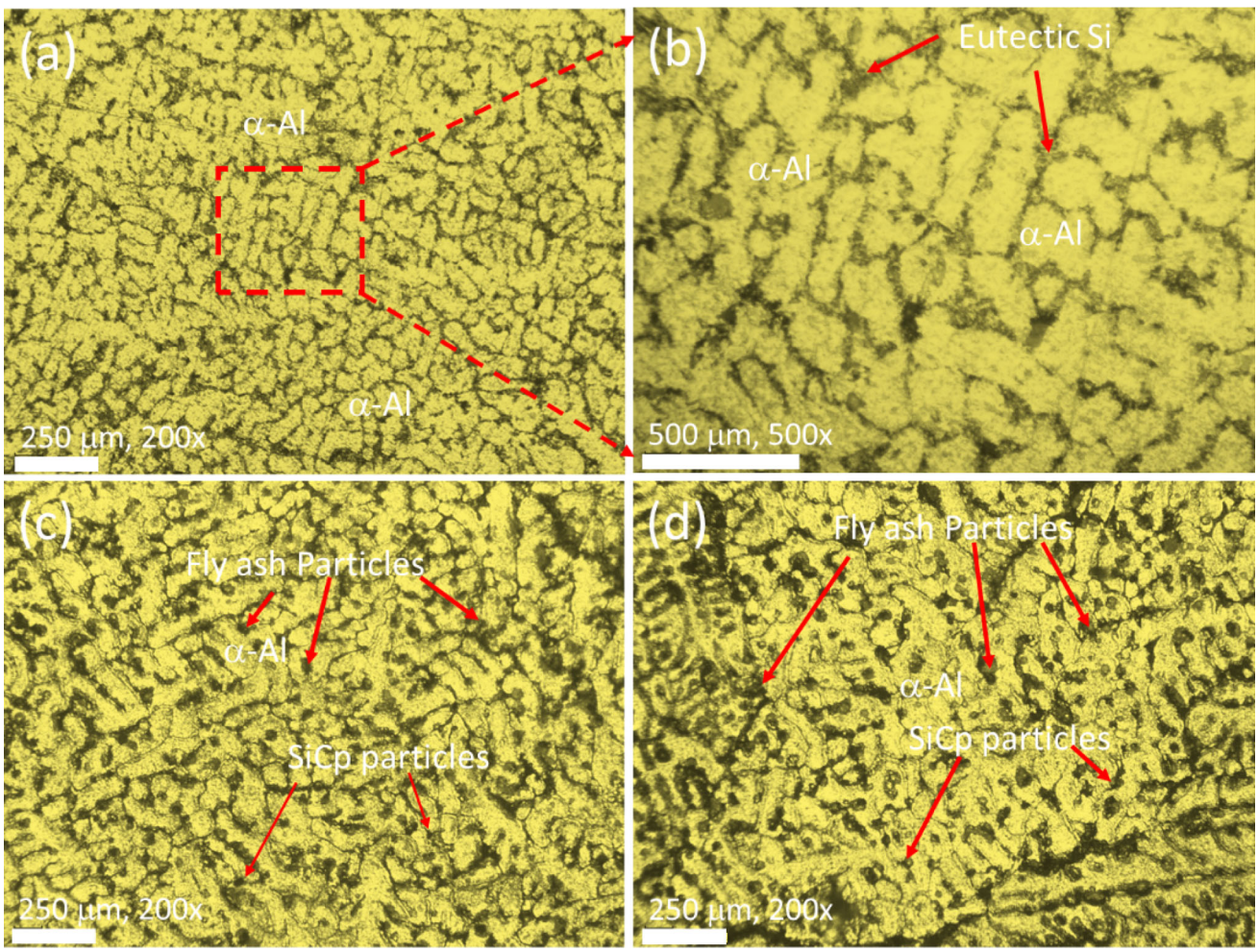

Figure 8. Optical microstructures of: (a) squeeze cast A356 alloy; (b) magnified image of (a); (c) squeeze cum stir cast A356-5 wt% fly ash-2.5SiC hybrid composite; (d) squeeze cum stir cast A356-10 wt% fly ash-2.5SiC hybrid composite.

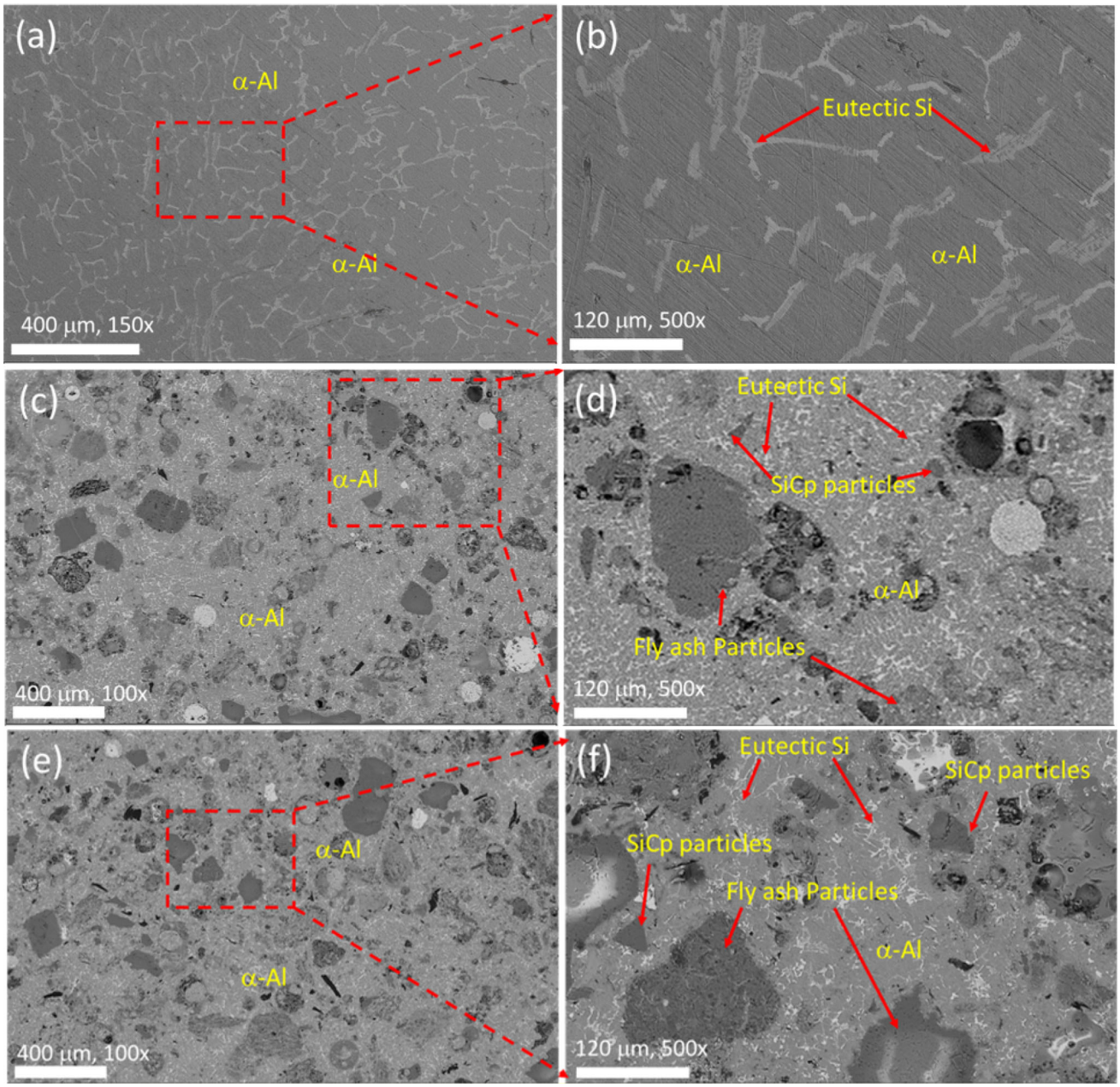

Figure 9. SEM microstructures of: (a) & (b) squeeze cast A356 matrix; (c) & (d) stir cum squeeze cast A356-5 wt% fly ash-2.5 wt% SiC hybrid composite; (c) stir cum squeeze cast A356-10 wt% fly ash-2.5 wt% SiC hybrid composite.

(Figure 10a, b). For quantification of squeeze cast A356 alloy chemical composition, spark optical emission spectrometer (Bruker, Germany) was used. Three samples were used in the spark OES and the average was used. The inset of Figure 10b illustrates the chemical composition of the squeeze cast A356 alloy which is within the theoretical limit as mentioned in Table 1. Figure 9c–f shows the α-Al, eutectic Si phases, along with uniform dispersion/bonding of incorporated fly ash and SiC particles. These results demonstrate the successful development of the hybrid composites. However, the observed fly ash particles in the hybrid composite was appearing like broken particles (having small pores) after squeezing due to cenospheres form (Figure 9d, f).[31] The wetting/adhesive nature of the SiCp ceramic reinforcements added to the matrix was expected to enhance the load transition between the reinforcements. Furthermore, based on microstructural examination, there was no sign of microporosity or defects in the casted samples owing to the use of the stir cum squeeze casting processing route which is expected to increase the mechanical strength.[32]

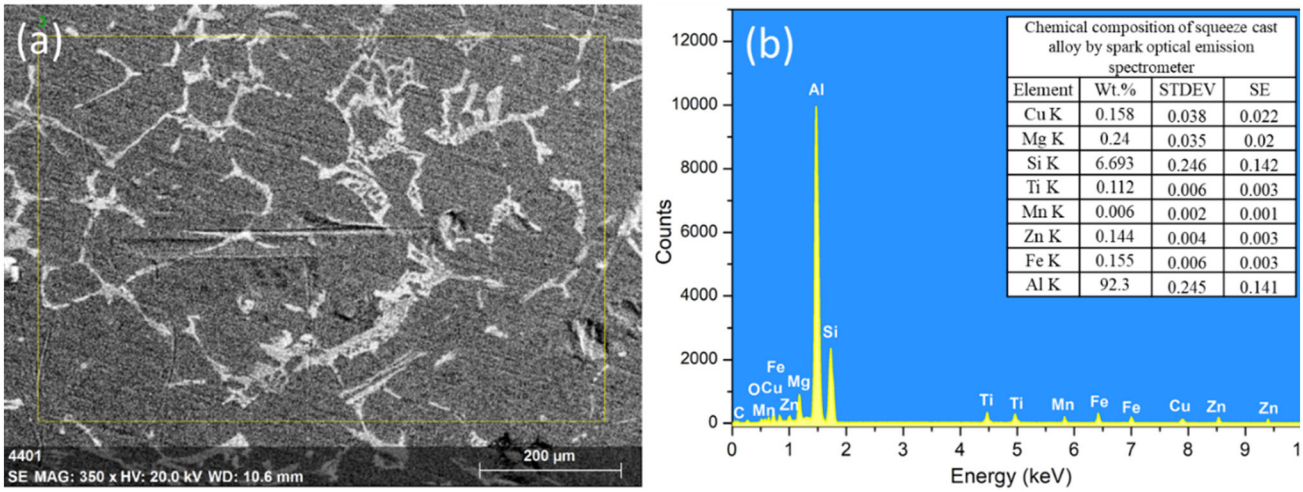

Figure 10. SEM energy dispersive spectrum of squeeze cast A356 alloy: (a) area of SEM microstructure for EDS; (b) corresponding spectrum. The inset of (b) indicate the chemical composition measured by spark optical emission spectrometer.

Table 3. Mechanical Properties of Squeeze Cast A356, Stir-Cum Squeeze Cast A356-(5, 10) wt% Fly ash-2.5wt%SiC Hybrid Composites

Samples	Yield strength, MPa	Ultimate tensile strength, g/cm^3	Elongation, %	Brinell Hardness, HB
A356 alloy	163 ± 4.86	288 ± 1.52	6.35 ± 1.25	76.58 ± 4.2
A356 + 5 wt% fly ash + 2.5 wt% SiC	184 ± 3.42	308 ± 1.45	2.85 ± 2.30	91.4 ± 2.7
A356 + 10 wt% fly ash + 2.5 wt% SiC	205 ± 3.65	329 ± 1.55	2.46 ± 1.65	98.35 ± 3.8

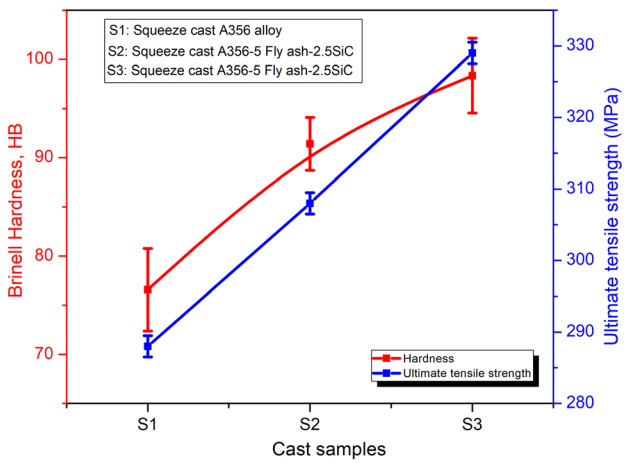

Figure 11. Variation in Brinell hardness and ultimate strength of squeeze cast A356 alloy, and A356 reinforced with fly ash and SiC hybrid composites.

Examination of Mechanical Behavior of Developed Hybrid Composites

The mechanical behavior by means of Brinell hardness and ultimate tensile strength of squeeze cast A356 matrix and stir cum squeeze cast A356-(5, 10) wt% fly ash-2.5wt%SiC hybrid composite samples were carried out (Table 3). With the inclusion of different wt% of fly ash and SiC particles in the matrix, the resulting hardness, yield strength, and tensile strength increased steadily. However, the ductility in terms of percentage elongation was started to decreases with increasing amount of fly ash and SiC particles. Hardness is referred to resistance against the indentation of the material. Figure 11 (left side *y*-axis) represents the average value of the Brinell hardness with an error bar. The corresponding measured average hardness was 76.58 ± 4.2HB, 91.4 ± 2.7 HB, and 98.35±3.8 HB for squeeze cast A356 matrix, stir cum squeeze cast A356-5wt% fly ash-2.5 wt% SiC, and A356-10wt% fly ash-2.5 wt% SiC hybrid composite samples respectively. The A356-10wt% fly ash-2.5 wt% SiC hybrid composite exhibited around 7.6%, and 28.4% higher than A356-5wt% fly ash-2.5 wt% SiC hybrid composite, and A356 alloy respectively. An increase in the hardness value was attributed to the mixing and embedding of fly ash and SiC particles over the A356 matrix (Figures 8 and 9).[26] In addition, the presence of higher wt% of fly ash particles in the A356 matrix led to more grain refinement with dislocations (Table 2, Figure 8),[7] and efficient bonding between the A356 matrix, fly ash, and SiC particles (Figure 9) which resulted in an improvement in the hardness value.[32,33] In addition, the applied load was passed to the reinforced particles, whenever the hybrid composite was indented by the indenter. Reinforced particles

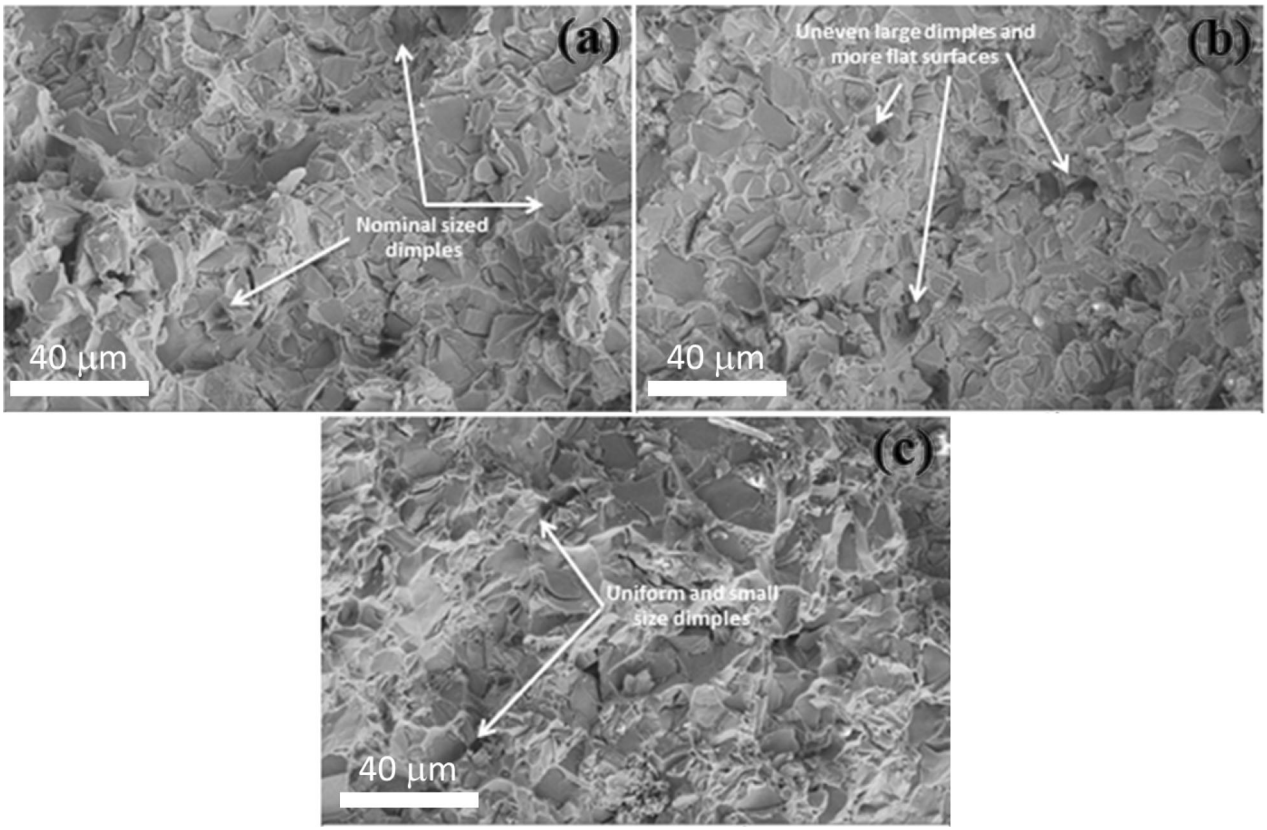

Figure 12. Fracture surface morphology of (a) squeezed A356 matrix, (b) stir cum squeeze cast A356-5 wt% fly ash-2.5 wt% SiC hybrid composite, (c) stir cum squeeze cast A356-10 wt% fly ash-2.5 wt% SiC hybrid composite.

not only sustain the applied load but also constrain plastic deformation geometrically. This produces geometrically required dislocations to withstand the deformation of the applied load. These dislocations contribute to the dislocation density of the composite, resulting in dislocation hardening. As a consequence, the hardness of the composites increased as the number of particles increased. The increase in hardness was due to dispersion strengthening, which enhanced the dislocation density and embedding of the incorporated SiCp and fly ash particles as a result of an effective load distribution mechanism. In addition, owing to proper blending and embedding of particles with a random distribution of higher wt% of fly ash reinforcement particles with increased densification (98.4%) due to squeezing.[34] In addition, the greater amount of resistance again plastic deformation was expected to be offered by the hard surface area of both SiC and fly ash particles leading to the production of pore-free fine surfaces. The highest tensile stress that a material can endure until failure is referred to as its ultimate tensile strength. Figure 11 (right side *y*-axis) depicts the average value of the ultimate tensile strength with an error bar. The average ultimate tensile strength values were 288MPa, 308 MPa, and 329MPa for the squeeze cast A356 matrix and stir cum squeeze cast A356-5 wt% fly ash-2.5 wt% SiC hybrid composite, and A356-10 wt% fly ash-2.5 wt% SiC hybrid composite respectively. Stir cum squeeze cast A356-10 wt% fly ash-2.5 wt% SiC hybrid composite experiences a 14.23% increase in the tensile strength over squeeze cast A356 matrix. This reveals that stir cum squeeze cast hybrid composite specimens have high tensile strength as a result of proper blending and embedding of higher wt% reinforcement particles over the A356 matrix, resulting in efficient load transfer due to hard particles serving as a shield for dislocation movement between the reinforcing particles and the A356 matrix.[35] The observed results also confirm that fly ash addition has a marginal impact on the strength of the composites.

Figure 12a–c depicts the fracture SEM images of the squeeze cast A356 matrix, stir cum squeeze cast A356-5 wt% fly ash-2.5 wt% SiC and A356-10 wt% fly ash-2.5 wt% SiC hybrid composites. Nominal sized dimples were observed in the squeeze cast A356 matrix (Figure 12a) indicating a more ductile and poor strength character. Uneven large dimples and flatter surfaces were observed in the stir-cum-squeezed A356 with 5 wt% fly ash and 2.5 wt% SiC hybrid composite (Figure 12b) indicating more strength characteristics. As a result, this sample exhibited less mechanical properties than A356 with 10 wt% fly ashes and 2.5 wt% SiCp hybrid composite sample. Owing to the increased weight percentage and uniform distribution

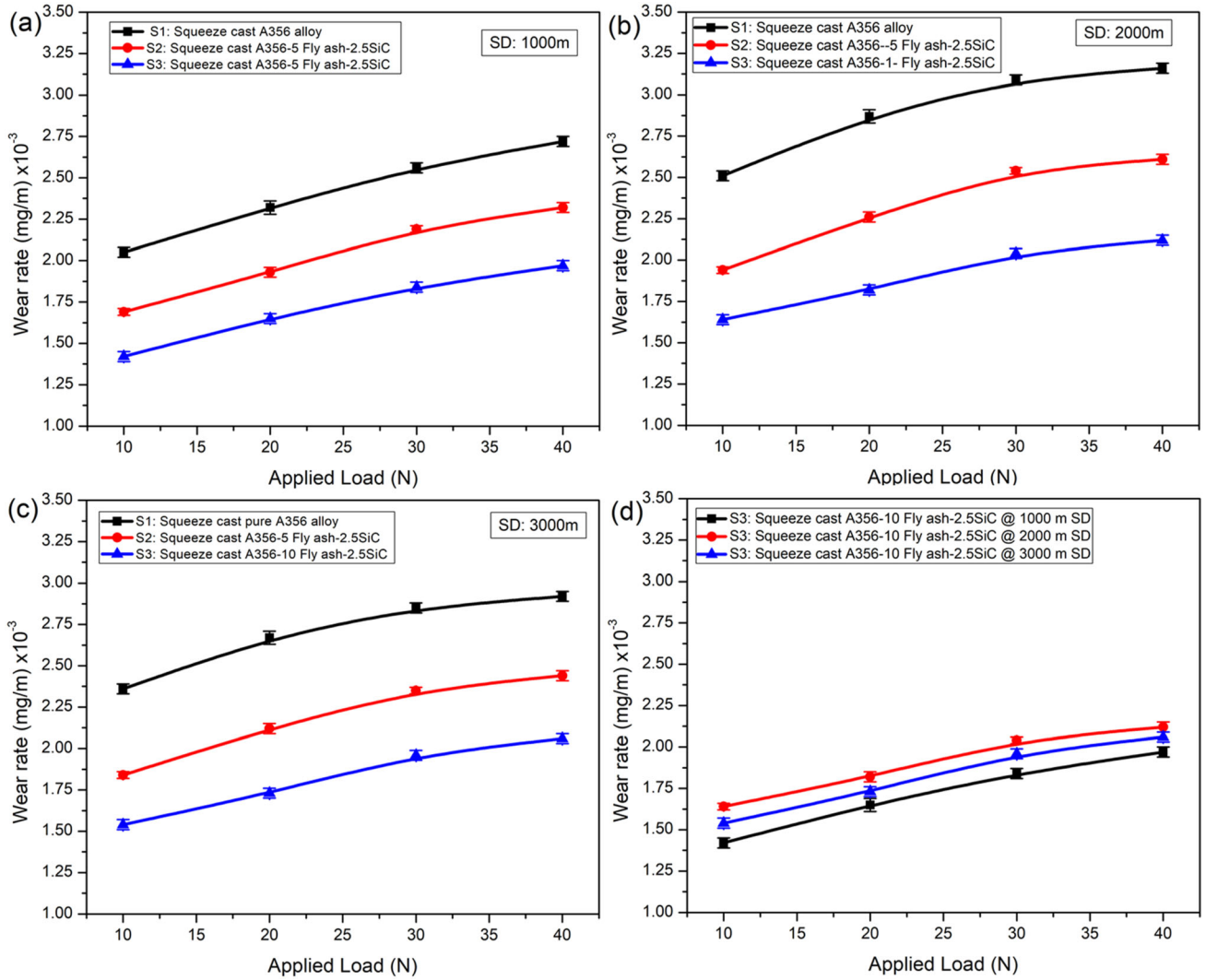

Figure 13. Variation of wear rate with the function of applied load at different sliding distances: (a) 1000 m; (b) 2000 m; and (c) 3000 m; (d) overall performance of A356-10 Fly ash-2.5SiC hybrid composite under various sliding conditions.

of fly ash and SiC particles (10 wt% fly ashes and 2.5 wt% SiCp) with enriched densification (>90%) caused by stir cum squeezing, identical and small-sized dimples were noticed in stir cum squeezed A356 with 10 wt% fly ash and 2.5 wt% SiC hybrid samples (Figure 12c). These results indicate that the stir cum squeezed A356 with 10 wt% fly ash and 5 wt% SiC hybrid composite sample exhibited a high tensile strength as a result of the efficient load transition of reinforcements in the matrix.

Examination of Tribological Properties

Wear Rate

Wear is the gradual deterioration of a part's surface caused by its motion to other operating parts. Therefore, wear should be reduced in real-time applications, particularly for critical automotive components. Figure 13a–c resembles the variation of wear rate of three prepared samples from low to top load variants of 10–40N at various sliding distance conditions of 1000–3000 m. From the investigation, it was observed that the stir cum squeeze cast A356-10 wt% fly ash-2.5 wt% SiC hybrid composite exhibited a lower wear rate with respect to both load and sliding conditions. This was due to the strong interfacial bonding, uniform distribution, and pore-free mechanical integrity between the fly ash and SiC particles with the A356 matrix.[21,33] Compared to the unreinforced A356 matrix, the hybrid composite samples exhibited a decrease in wear rate owing to the presence of fly ash and SiC particles. The efficient interfacial bonding and enhanced densification (> 98%) due to stir cum squeezing along with better hardness and strength are also responsible for the lower wear rate of the stir-cum squeeze cast A356-10 wt% fly ash-2.5 wt% SiC hybrid composite.[33] Furthermore, because of the soft nature and lower weight percentage of fly ash and SiC particles in the matrix, the squeeze cast A356 matrix and

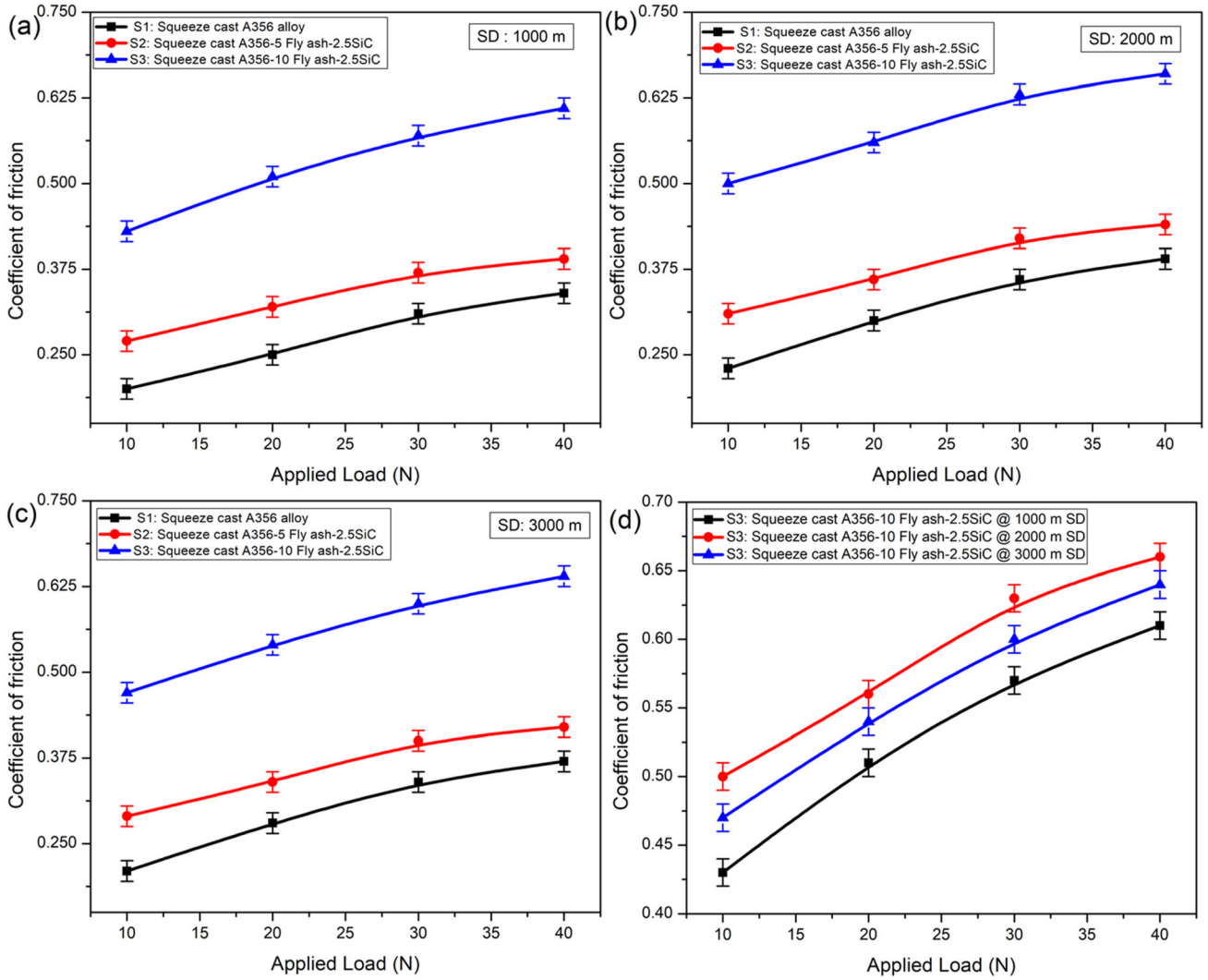

Figure 14. Variation of coefficient of friction with the function of applied load at different sliding distances: (a) 1000 m; (b) 2000 m; and (c) 3000 m; (d) overall performance of A356-10 Fly ash-2.5SiC hybrid composite under various sliding conditions.

stir cum squeeze cast A356-5 wt% fly ash-2.5 wt% SiC hybrid composite samples produced higher and moderate wear rates. As a result, the wear rates increased with the increase in load and sliding distance. When the load applied was minimal, the wear rate was observed to be lower with less debris, however, when the load was increased, the volume of material removed increased because of the increased rubbing action in the form of debris.[36] Additionally, the hybrid composite sample with a higher weight percentage addition produced a lower wear rate owing to the addition of the hard phase of fly ash and SiC reinforcement particles with the A356 matrix processed by the stir-cum squeeze casting route resulting in mild debris formation due to better pore-free interfacial bonding followed by higher hardness and strength.[33,37,38] For the lower sliding distance conditions of 1000m, the wear rate observed was minimal, and it resembled gentle scratches accompanied by abrasion and delamination caused by mild direct metal to metal contact. At an intermediate sliding distance of 2000 m, the improved travel time enabled more direct metal-to-metal interaction, resulting in particle weakening and delamination and a moderate wear rate. The wear rate continues to decrease when moving at an extreme sliding distance of 3000 m as a result of hardening of both the pin and counter disc surfaces, accompanied by the softening nature of all test materials. As seen in Figure 13d, the wear rate increased linearly up to 2000m sliding distance and then decreased to 3000 m for all the test samples. Overall, stir cum squeeze cast A356-10 wt% fly ash-2.5 wt% SiC hybrid composite exhibited a lower wear rate owing to better metallurgical and mechanical properties. At a 40N load and 3000m sliding distance, the stir-cum squeeze cast A356-10 wt% fly ash-2.5 wt% SiC hybrid composite exhibited a wear rate reduction of approximately 41.74% when compared to the squeeze cast A356 matrix.

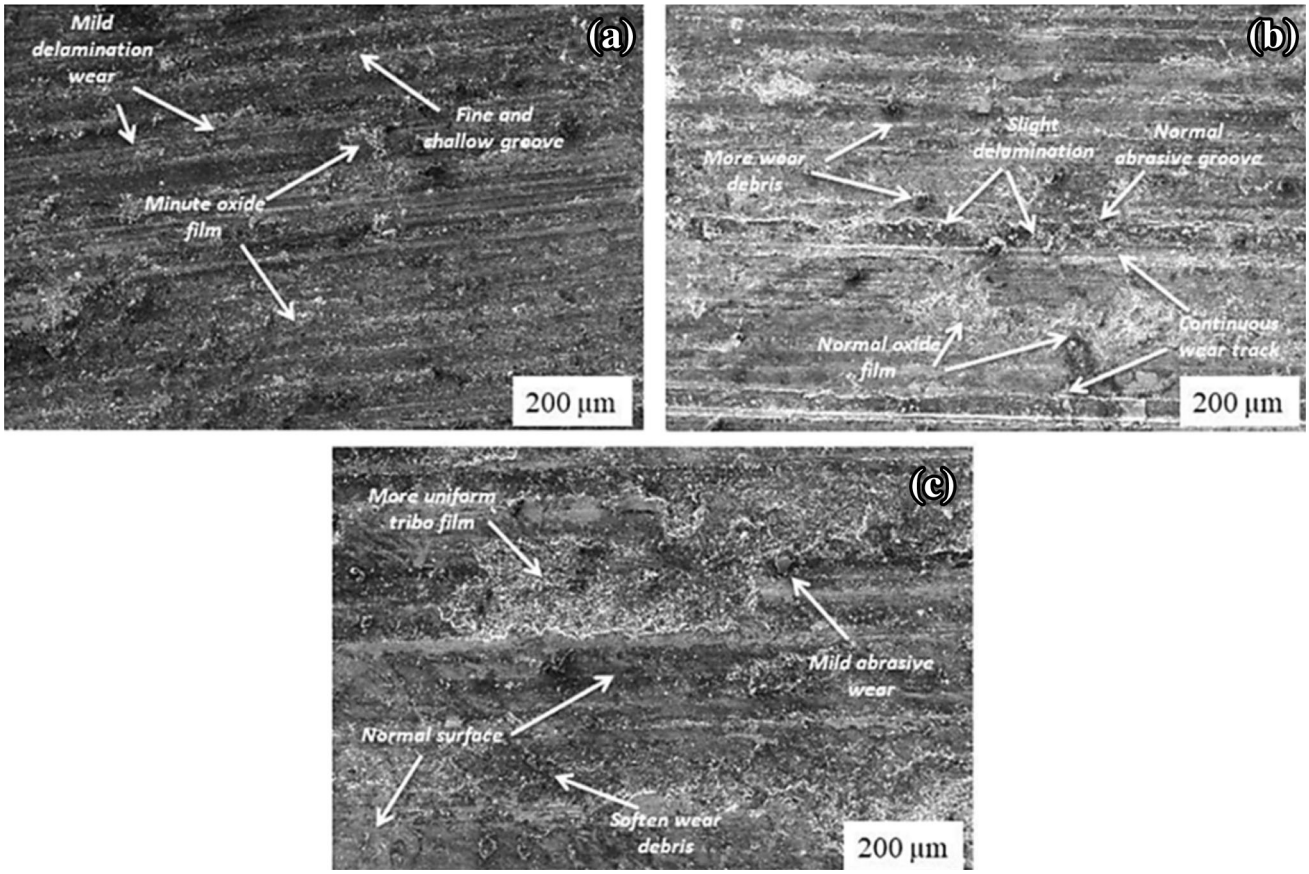

Figure 15. SEM micrographs of the worn-out surfaces of stir cum squeeze cast A356-10 wt% fly ash-2.5 wt% SiC hybrid composites: (a) at a Load of 10 N and sliding distance of 1000 m (b) at a Load of 10 N and sliding distance of 2000m (c) at a Load of 10 N and sliding distance of 3000 m.

Friction Coefficient

The friction coefficient is described as the relationship between friction force and applied load. Figure 14a–c shows the deviation in frictional coefficient values between the squeeze cast A356 matrix and stir cum squeeze cast A356-x (5,10) wt% fly ash-2.5 wt% SiC hybrid composites from low to top load conditions of 10–40N at different sliding distances (1000 to 3000m). The results revealed that at a 10N load, the friction coefficient of the specimen was low with fly ash and SiC hybridization, but when the load increases from 10N to 40N, the friction coefficient was high and exhibited greater values owing to the combined effect of reinforcement addition and stir cum squeeze casting processing route, thus, a greater frictional force was needed when sliding over the rotating disc. This occurs because the pin surface asperities are caught by the rotating disc, resulting in abrasions with increased surface roughness.[38] Furthermore, the friction coefficient increases for castings at sliding distances of 2000m as compared to 1000m and 3000m. In general, for the low sliding distance condition (1000 m), the friction coefficient was expected to be low and small scratches were introduced when there was a mild direct metal to metal contact. However, at an intermediate sliding distance of 2000 m, the abrasives in conjunction with the specimen deteriorated owing to the prolonged running period. Consequently, the formation of a continuous and strong mechanically mixed layer or oxide film between the pin surface and the steel counter face disappeared.[39,40] This occurs at the contact surface as the sliding distance increases from 1000m to 2000m due to the temperature increase, resulting in an improved friction coefficient. At a higher sliding distance of 3000m, the interfacial temperature allowed the formation of a dense oxide layer and material softening, resulting in a small reduction in the coefficient of friction (Figure 14d).[41,42] In comparison to other cast specimens, the stir cum squeeze cast A356-10 wt% fly ash-2.5 wt% SiC hybrid composite exhibited a higher friction coefficient. This results from the increase in the friction force as the mechanical strength increases. However, the lower frictional force results in a diminishing rate in the friction coefficient for the squeeze cast A356 matrix and stir cum squeeze cast A356-5wt% fly ash-2.5wt%SiC hybrid composite due to the matrix material's soft nature with greater plastic flow containing fewer reinforcements with matrix alloy than the stir cum squeeze cast A356-10wt% fly ash-2.5wt%SiC hybrid composite. Quantitatively, the friction coefficient of the stir-cum squeeze cast A356-10wt% fly ash-2.5wt%SiC hybrid

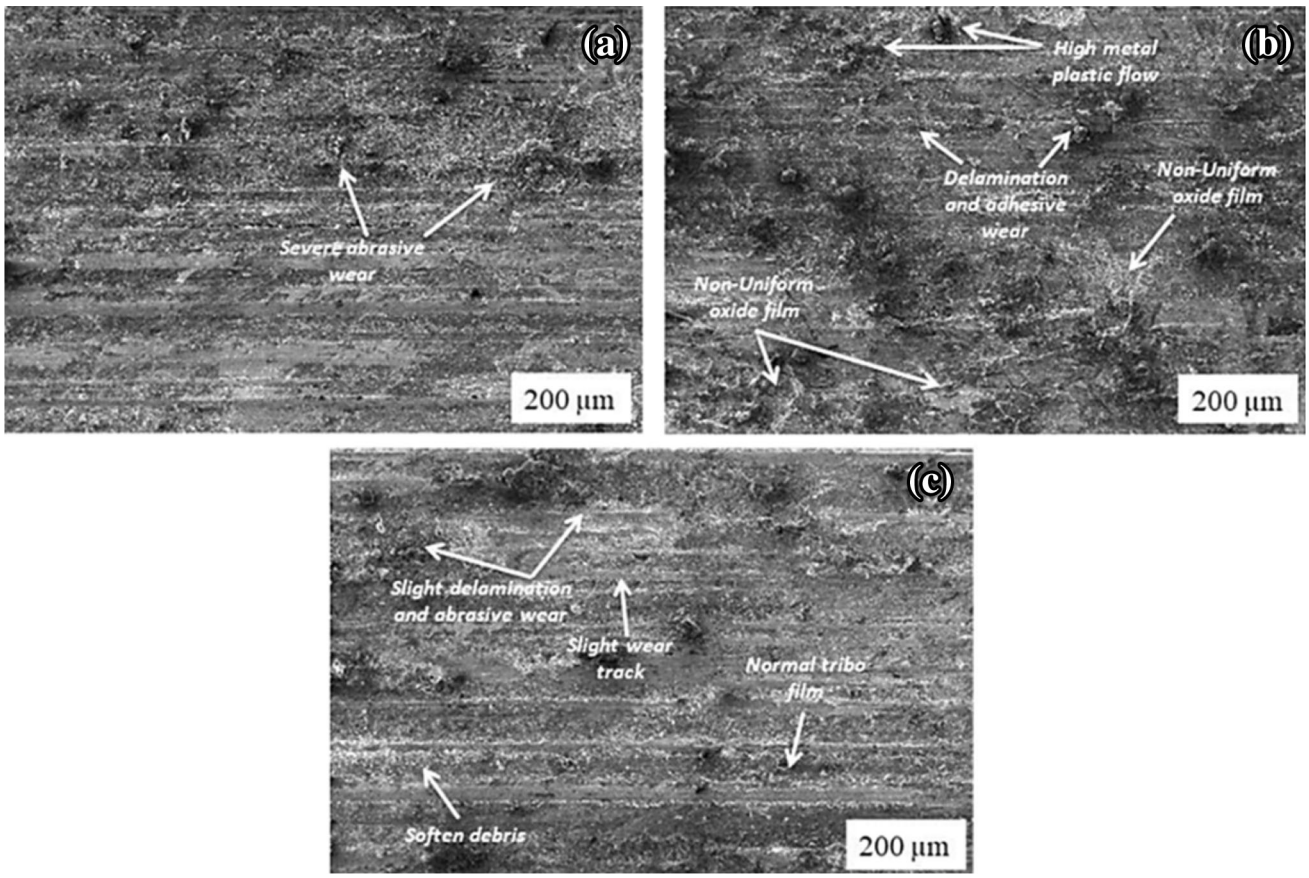

Figure 16. SEM micrographs of the worn-out surfaces of stir cum squeeze cast A356-10 wt% fly ash-2.5 wt% SiC hybrid composites: (a) at a Load of 40 N and sliding distance of 1000 m (b) at a Load of 40 N and sliding distance of 2000 m (c) at a Load of 40 N and sliding distance of 3000 m.

composite produced 72.97% greater than that of squeeze cast A356 matrix for 40N load and 3000 m sliding distance.

Worn Surface Analysis

Stir cum squeeze cast A356-10 wt% fly ash-2.5 wt% SiC hybrid composite exhibits improved physical, metallurgical, mechanical, and tribological behavior. To confirm that, worn surfaces were verified by SEM investigation. The worn surfaces of the stir-cum squeeze cast A356-10 wt% fly ash-2.5wt%SiC hybrid composite are depicted in Figures 15 and 16. As shown in Figure 15a, when a load of 10N was applied and at a sliding distance of 1000m, fine and shallow grooves were found on the worn sub-surface as a result of radical delamination. Additionally, a minute province of the oxidized film was detected as a result of a slightly elevated interface temperature between the pin and disc.[41] From Figure 15b, it can be seen that, at a sliding distance of 2000m and an applied load of 10N, the number of normal abrasive grooves increased in the subsurface with a continuous wear track and slightly delaminated from the pin surface owing to rubbing actions. As a result, the formation of additional wear debris was found between the counter face and pin at a continuously higher travel time, and because a normal oxide tribo film was formed. Furthermore, Figure 15c shows that there was no flack detachment or propagation of cracks within the worn surface, indicating that only identical mild abrasive wear and a normal surface occurred as a result of the effective load-bearing capacity provided by the even distribution of fly ash and SiC particles. Furthermore, there was enriched densification due to squeezing, thereby leading to decreased damage in the worn surface of the hybrid composites, and a more uniform tribo oxide film and softened wear debris were observed in the low load condition of 10N and a higher sliding distance of 3000m.[29,43]

The worn surface of the stir-cum squeeze cast A356-10 wt% fly ash-2.5 wt%SiC hybrid composite at 40N of higher load and 1000m low sliding distance is depicted in Figure 16a. As a result of the extreme pressure at the contact surface, excessive abrasive wear occurred, resulting in the removal of metal flow in the wear track. As shown in Figure 16b, at an applied load of 40 N for sliding distance up to 2000m, extreme delamination and adhesion wear were observed on the worn surfaces leading to excessive plastic deformation, which resulted in the development of a non-uniform oxide film on the worn surface. The wear at the contact surface at a higher sliding distance of 3000m

and a load of 40N is depicted in Figure 16c, where greater surface stress occurred in the specimen owing to the long travel distance and load, resulting in the formation of slight delamination and abrasive wear. This may be caused by the absence of flakes and de-bonding on the worn surfaces.[21] Additionally, the increased contact pressure at the specimen-disc interface over a long run sliding distance resulted in the visibility of a slight wear track with softened wear debris and a regular tribo film.

From the investigation, it is evident that for all load conditions at a lower sliding distance of 1000m, there was a slight disruption as a result of the specimen's reduced surface stress and reduced contact distance/duration. After 2000 m sliding distance, slight delamination and abrasion, accompanied by a regular tribo film was observed on the worn surface of the stir-cum squeeze cast A356-10 wt% fly ash-2.5 wt% SiC hybrid composite, and a lower wear rate were observed at 3000 m sliding distance than 2000 m sliding condition. Additionally, the reported physical, metallurgical, mechanical, and tribological responses confirmed that increasing the weight percentage of fly ash particles accompanied by squeezing results in a pore-free fine-grain distribution with improved particle bonding in the matrix phase. Thus, an improved wear mechanism was observed on a stir cum squeeze cast A356-10 wt% fly ash-2.5 wt%SiC hybrid composite due to better bonding, densification, higher hardness, and strength.

Conclusions

The physical, metallurgical, mechanical, and tribological properties of an A356 hybrid composite reinforced with fly ash and SiC were investigated in this study and the findings are summarized as follows:

- Squeeze cast A356 and A356 with *x* (5, 10) wt% fly ash and 2.5 wt% SiC hybrid composite were successfully fabricated by a stir cum squeeze casting process. The density of the stir-cum squeeze cast A356-10wt% fly ash-2.5 wt% SiC hybrid composite was found to be lower (2.38 g/cm^3) than the other cast samples. Uniform distribution of fly ash and SiC particles in the matrix and pore-free better bonded hybrid composites were produced owing to the effect of squeeze pressure.
- X-ray diffraction results revealed the presence of α-Al, eutectic Si, incorporation of fly ash and SiC particles in the hybrid composites.
- Metallography analysis through optical microscopy and SEM revealed the presence of α-Al, eutectic Si, fly ash particles, and SiC particles with pore-free and uniform distribution of particles tightly bonded inside the matrix. Effective bonding between matrix with fly ash and SiC particles as well as applied squeeze pressure enhances a higher recorded value of hardness and strength of stir cum squeeze cast A356-10 wt% fly ash-2.5wt%SiC hybrid composite.
- Stir cum squeeze cast A356-10 wt% fly ash-2.5 wt% SiC hybrid composite possessed the least wear rate and higher friction coefficient in aspects of both loaded and sliding conditions due to improved metallurgical and mechanical properties. The rate of wear and friction coefficient rapidly increased as the applied load rises from 10N to 40N and at different sliding distances between 1000 and 2000 m. Owing to the formation of a tribo layer on the interface, the wear rate was lower for a longer span of 3000 m sliding distance than for 2000 m sliding distance.
- Worn surface SEM analysis revealed that an adequate level of damage was observed under higher load and sliding distance conditions resulting from high contact pressure at the specimen-disc interface leading to a slight wear track with softened wear debris and normal tribo film.
- Overall, a lower wear rate and higher value of friction coefficient were observed for all the test trails in the stir cum squeeze cast A356-10 wt% fly ash-2.5 wt% SiC hybrid composite. Owing to the enriched properties, the stir-cum squeeze cast A356-10 wt% fly ash-2.5 wt% SiC hybrid composite was recommended as an alternate material in automotive industries.

Abbreviations

A/Al	Aluminum
AMCs	Aluminum matrix composites
HMMCs	Hybrid metal matrix composites
B_4C	Boron carbide
Al_2O_3	Aluminium oxide
SiC	Silicon carbide
Gr	Graphite
AIN	Aluminium nitride
TiB_2	Titanium boride
ZrO_2	Zirconium oxide
°C	Degree Celsius
ASTM	American Society for Testing and Materials
SiO_2	Silicon dioxide
Fe_2O_3	Iron oxide
Mg	Magnesium
Ca	Calcium
Na	Sodium
K	Potassium

Authors' contributions RS: Conceptualization, Methodology, Formal Analysis; AS: Investigation, writing—original draft preparation; SS: Data curation, Writing-review and editing; GS: Methodology, Formal analysis; SK: Data curation, and conceptualization.

Availability of Data and Material

The experimental datasets obtained from this research work and the analyzed results during the current study are available from the corresponding author on reasonable request.

Conflict of Interest The authors declare no financial or commercial conflict of interest.

Ethics Approval The submitted work is original and is not published elsewhere in any form.

REFERENCES

1. X. Liu, S. Jia, L. Nastac, Int. J. Met. **8**, 51–58 (2014)
2. C.Y. Liu, B. Zhang, Z.Y. Ma, H.J. Jiang, W.B. Zhou, J. Alloys Compd. **772**, 775–781 (2019)
3. M. Asif, K. Chandra, P.S. Misra, J. Miner. Mater. Charact. Eng. **10**, 1337–1344 (2011)
4. P.B. Madakson, D.S. Yawas, A. Apasi, Int. J. Eng. Sci. Technol. **4**, 1190–1198 (2012)
5. M.O. Bodunrin, K.K. Alaneme, L.H. Chown, J. Mater. Res. Technol. **4**, 434–445 (2015)
6. K.K. Alaneme, P.A. Olubambi, J. Mater. Res. Technol. **2**, 188–194 (2013)
7. H. Tahiri, S.S. Mohamed, H.W. Doty, S. Valtierra, F.H. Samuel, Int. J. Met. **12**, 343–361 (2018)
8. A.K. Kasar, N. Gupta, P.K. Rohatgi, P.L. Menezes, Jom **72**, 2340–2351 (2020)
9. P.K. Rohatgi, J.K. Kim, N. Gupta, S. Alaraj, A. Daoud, Compos. Part A Appl. Sci. Manuf. **37**, 430–437 (2006)
10. S. P. Dwivedi, S. Sharma, R. K. Mishra, Int. J. Manuf. Eng. **2014**, 1–13
11. S. P. Dwivedi, S. Sharma, R. K. Mishra, Microstructure and mechanical behavior ofA356/SiC/Fly-ash hybrid composites produced by electromagnetic stir casting (Retraction of Vol 37, art no 57, 2015), (2020).
12. X. Canute, M.C. Majumder, J. Eng. Sci. Technol. **13**, 755–777 (2018)
13. A. Vencl, I. Bobic, S. Arostegui, B. Bobic, A. Marinković, M. Babić, J. Alloys Compd. **506**, 631–639 (2010)
14. A. Karthikeyan and S. Nallusamy, in International Journal of Engineering Research in Africa, Trans Tech Publ, 2017, vol. 31, pp. 36–43
15. H.R. Lashgari, S. Zangeneh, H. Shahmir, M. Saghafi, M. Emamy, Mater. Des. **31**, 4414–4422 (2010)
16. R. Suresh, M.P. Kumar, Int. J. Res. Eng. Technol. **1**, 91–104 (2013)
17. R. Palanivel, I. Dinaharan, R.F. Laubscher, J.P. Davim, Mater. Des. **106**, 195–204 (2016)
18. B.A. Kumar, N. Murugan, I. Dinaharan, Trans. Nonferrous Met. Soc. China **24**, 2785–2795 (2014)
19. G. Karthikeyan, G.R. Jinu, Trans. FAMENA **39**, 89–98 (2015)
20. P. Sharma, D. Khanduja, S. Sharma, J. Mater. Res. Technol. **5**, 29–36 (2016)
21. R. Soundararajan, S. Sivasankaran, F.A. Al-Mufadi, M. Akilesh, P.R. Elango, Mater. Res. Express **6**, 96572 (2019)
22. V.S. Ayar, M.P. Sutaria, Development and Characterization of In Situ AlSi5Cu3/TiB2 Composites. Int. J. Met. **14**, 59–68. https://doi.org/10.1007/s40962-019-00328-x (2020)
23. R.K. Uyyuru, M.K. Surappa, S. Brusethaug, Wear **260**, 1248–1255 (2006)
24. N. Radhika, R. Subramanian, S. V. Prasat, B. Anandavel, Ind. Lubr. Tribol. **64**, 359–366
25. H. Ghandvar, S. Farahany, M.H. Idris, Tribol. Trans. **61**, 88–99 (2018)
26. I. A. Alkadir, L. S. Salim, Eng. Technol. J. **26**, 301–310
27. V.S. Aigbodion, S.B. Hassan, Mater. Sci. Eng. A **447**, 355–360 (2007)
28. A. Mohammed Razzaq, D. L. Majid, M. R. Ishak, U. M. Basheer, Metals (Basel), 2017, **7**, 477.
29. M.S. Kumar, M. Vasumathi, S.R. Begum, S.M. Luminita, S. Vlase, C.I. Pruncu, J. Mater. Res. Technol. **15**, 1201–1216 (2021)
30. B. Vinod, S. Ramanathan, M. Anandajothi, SN Appl. Sci. **1**, 1–15 (2019)
31. C. Wang, J. Liu, H. Du, A. Guo, Ceram. Int. **38**, 4395–4400 (2012)
32. U. Aybarç, O. Ertuğrul, M.Ö. Seydibeyoğlu, Int. J. Met. **15**, 638–649 (2021)
33. R. Gecu, A. Karaaslan, Tribol. Lett. **65**, 1–15 (2017)
34. S. Sivasankaran, K. R. Ramkumar, H. R. Ammar, F. A. Al-Mufadi, A. S. Alaboodi and O. M. Irfan, *J. Mater. Process. Technol.* https://doi.org/10.1016/j.jmatprotec.2021.117063.
35. A. Gnanavelbabu, K. T. S. Surendran, S. Kumar, Process Optimization and Studies on Mechanical Characteristics ofAA2014/Al2O3 Nanocomposites Fabricated Through Ultrasonication Assisted Stir–SqueezeCasting. Int. Met., 2021, 1–24. https://doi.org/10.1007/s40962-021-00634-3 (2021)
36. R. Gecü, A. Karaaslan, Tribol. Trans. **62**, 249–261 (2019)
37. D. M. Shinde, P. Sahoo, Influence of Speed and Sliding Distance on the Tribological Performance of SubmicronParticulate Reinforced Al-12Si /1.5 Wt% B4C Composite Int. J. Met., 2021, 1–20. https://doi.org/10.1007/s40962-021-00636-1 (2021)
38. R. Gecu, A. Karaaslan, Int. J. Met. **13**, 641–652 (2019)
39. K. Nithesh, M. C. Gowrishankar, R. Nayak, S. Sharma, J. Mater. Res. Technol. **15**, 4272–4292
40. V. Verma, R.C. Cozza, V. Cheverikin, A. Kondratiev, R. Penchaliah, SN Appl Sci. **3**, 1–13 (2021)
41. N. Radhika, J. Sasikumar, J.L. Sylesh, R. Kishore, J. Mater. Res. Technol. **9**, 1578–1592 (2020)
42. H. Xie, Y. Cheng, S. Li, J. Cao, C.A.O. Li, Trans. Nonferrous Met. Soc. China **27**, 336–351 (2017)

43. M. Zolfaghari, M. Azadi, M. Characterizationof High-Cycle Bending Fatigue Behaviors for Piston Aluminum Matrix SiO2 Nano-composites inComparison with Aluminum–Silicon Alloys. Azadi, Int. J. Met. **15**, 152–168 https://doi.org/10.1007/s40962-020-00437-y (2021).